

-- Electronic Supplementary Information --

Understanding the Sigmatropic Shifts of Cyclopenta-2,4-dien-1-yltrimethylsilane in its Diels-Alder Addition

*Min Zhang,¹ Guangchao Liang^{*2}*

¹Department of Chemistry, Mississippi State University, Mississippi State, Mississippi 39762, United States

²Department of Chemistry, University of Michigan, Ann Arbor, Michigan 48109, United States

Table of Contents

Computational Methods.....	S3
Figure S1. The free energy diagram for various species in the conversion of 1-(C ₅ H ₅)Ge(Me) ₃	S4
Figure S2. The HOMO of isomers 1, 2 and 3.....	S4
Scheme S1. The resonance structures of isomer 1.....	S5
Scheme S2. The resonance structures of isomer 2.....	S5
Scheme S3. The resonance structures of isomer 3.....	S5
Figure S3. Computed paths for the proton shift in the conversion of cyclopenta-1,3-diene.....	S6
Figure S4. Computed paths for the proton shift in the conversion of 1H-pyrrol-1-ium	S6
Figure S5. The matched DFT optimized structures with reported X-ray crystal structures (Color green).	S7
Scheme S4. The second path of Diels-Alder addition of isomer 3 with TMSBO.	S7
Scheme S5. The second path of Diels-Alder addition of isomer 1 with TMSBO.	S8
Scheme S6. The path of Diels-Alder addition of isomer 2 with TMSBO.	S8
Table S1. Computed and experimental proton chemical shifts of 1-(C ₅ H ₅)Si(Me) ₃ at variable temperatures.....	S9
Figure S6. Comparisons of the computed proton chemical shifts and experimental ¹ H NMR of 1-(C ₅ H ₅)Si(Me) ₃	S9
Figure S7. IRC plots for the proton shift in the conversion of cyclopenta-1,3-diene.	S10
Figure S8. IRC plots for the silicon migration and proton shift in the conversion of 1-(C ₅ H ₅)Si(Me) ₃ . ..	S10
Figure S9. IRC plots for the formation of products a, b, c and d from Diels-Alder addition.	S11
Table S2. The selected molecular orbitals of proton shift TS-1 in cyclopenta-1,3-diene.....	S11
Table S3. The selected molecular orbitals of proton shift TS-1-i in cyclopenta-1,3-diene.	S11
Table S4. DFT optimized structures of 1-(C ₅ H ₅)Si(Me) ₃	S12
Table S5. The computed relative Gibbs free energies and electronic energies (parentheses) of 1-(C ₅ H ₅)Si(Me) ₃	S12
Table S6. The selected molecular orbitals of silicon migration TS-1-1 in 1-(C ₅ H ₅)Si(Me) ₃	S13

Table S7. The selected molecular orbitals of proton shift TS-1-2 in 1-(C ₅ H ₅)Si(Me) ₃	S13
Table S8. The selected molecular orbitals of proton shift TS-1-2-i in 1-(C ₅ H ₅)Si(Me) ₃	S13
Table S9. The computed relative Gibbs free energies and electronic energies (parentheses) of 1-(C ₅ H ₅)Ge(Me) ₃	S14
Table S10. DFT computed energies for species in Figures 1 and 2.....	S14
References.....	S15

Computational Methods

Gas-phase geometry optimizations were carried out via Gaussian 16 package (Revision C 01)¹ with PBEPBE²⁻³ functional and the Ahlrichs Def2-TZVP⁴⁻⁵ basis sets. Grimme's D3⁶ dispersion with Becke-Johnson damping (D3BJ)⁷ and automatic density fitting approximation⁸⁻⁹ (keyword AUTO) with pure spherical harmonic 5d and 7f functions were utilized for all optimization and SMD solvation computations. The vibrational frequency computations were used to verify the natures of all stationary points. All located transition states were obtained with only one imaginary frequency, and minima without any imaginary frequencies were obtained. The IRC (intrinsic reaction coordinate) computations from the located transition states were performed, and both directions of the reaction path following the transition state were computed (see ESI for the IRC plots). The Gaussian 16 default ultrafine integration grid, 2-electron integral accuracy of 10⁻¹², and SCF convergence criterion of 10⁻⁸ were used for all computations. The self-consistent reaction field (SCRF) single-point computations in benzene using the solvation model based on density (SMD)¹⁰ were used to model the solvation effects [SMD-PBEPBE-D3BJ/Def2-TZVP//PBEPBE-D3BJ/Def2-TZVP]. All computations were performed at 1 atm and 298.15 K. The molecular orbitals were generated by Multiwfn package (version 3.7)¹¹⁻¹² and VMD package (version 1.9.3)¹³⁻¹⁴. The 3D molecular structures were created via Cambridge Structural Database (CSD) Mercury package (version 4.0.0)¹⁵⁻¹⁶. NMR (nuclear magnetic resonance) computations (PBEPBE-D3BJ/Def2-TZVP) were carried out using Gauge-Independent Atomic Orbital (GIAO)¹⁷⁻¹⁹ method based on the gas-phase optimized geometry. All simulated proton chemical shifts were relative to the computed absolute shift of TMS (tetramethylsilane, 31.21 ppm at the level of PBEPBE-D3BJ/Def2-TZVP).

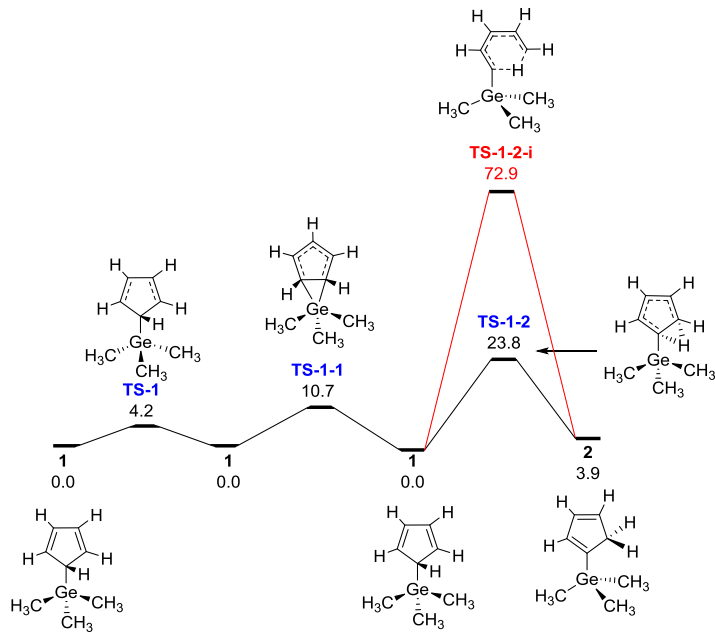


Figure S1. The free energy diagram for various species in the conversion of 1-(C₅H₅)Ge(Me)₃. Gibbs energies from (SMD)-PBEPBE-D3BJ/Def2-TZVP//PBEPBE-D3BJ/Def2-TZVP computations are given in kcal/mol.

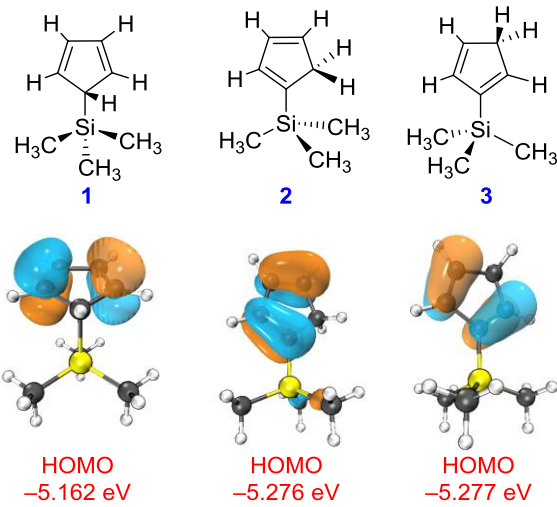
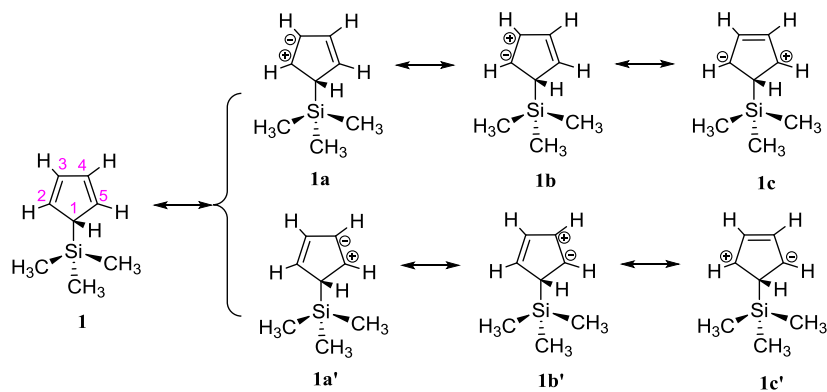
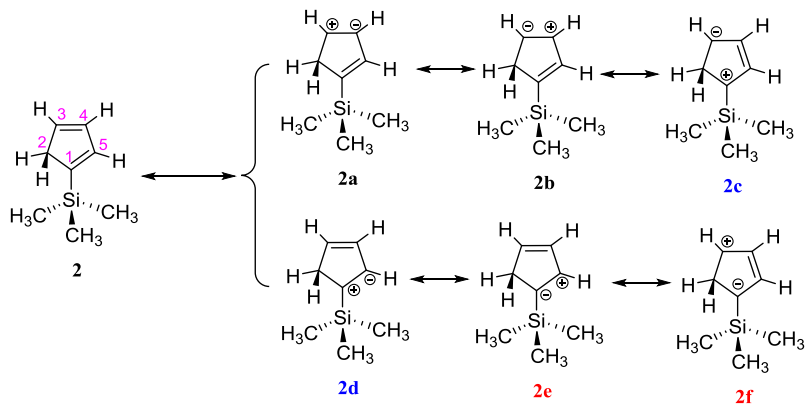


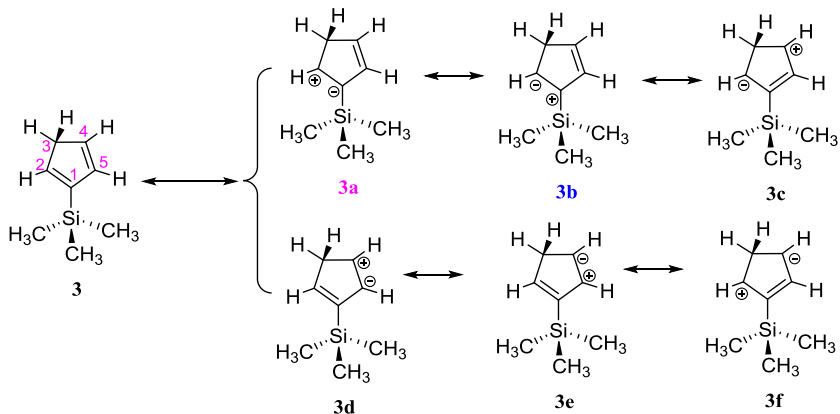
Figure S2. The HOMO of isomers 1, 2 and 3.
Isovalue=0.05. Color codes for 3D structures: black, C; white, H.



Scheme S1. The resonance structures of isomer **1**.



Scheme S2. The resonance structures of isomer **2**.



Scheme S3. The resonance structures of isomer **3**.

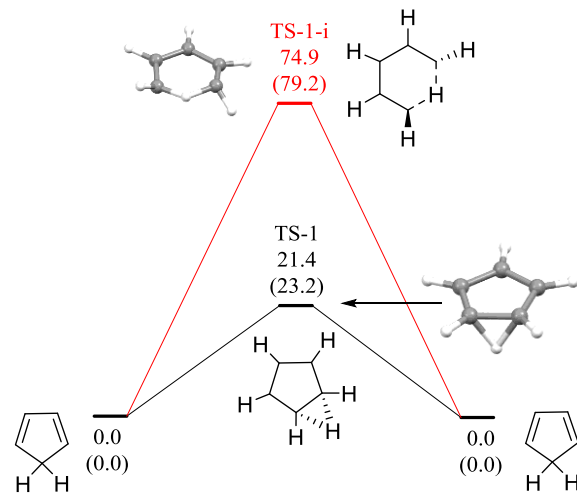


Figure S3. Computed paths for the proton shift in the conversion of cyclopenta-1,3-diene. The PBEPBE-D3BJ/Def2-TZVP computed gas-phase Gibbs free energies and electronic energies (parentheses) are given in kcal/mol.

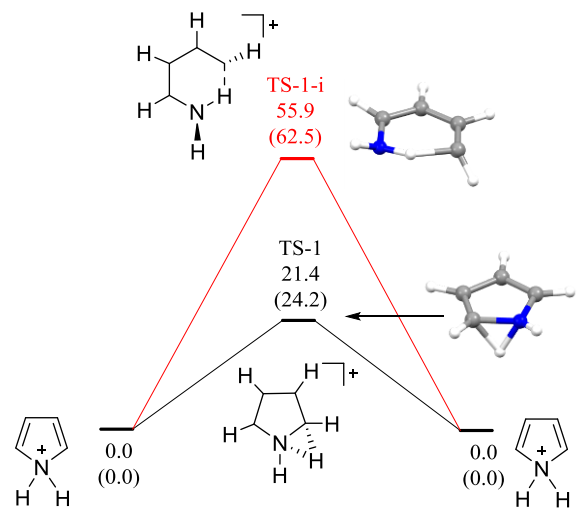


Figure S4. Computed paths for the proton shift in the conversion of 1H-pyrrol-1-i um. The PBEPBE-D3BJ/Def2-TZVP computed gas-phase Gibbs free energies and electronic energies (parentheses) are given in kcal/mol.

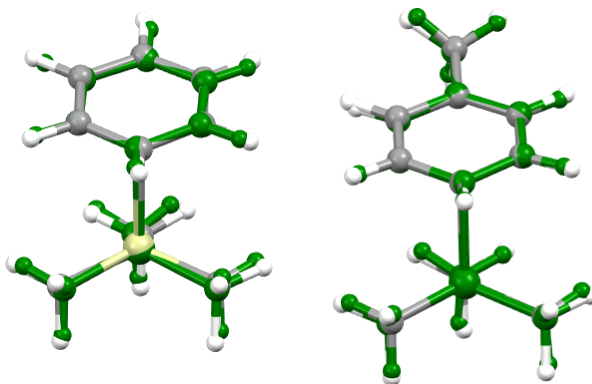
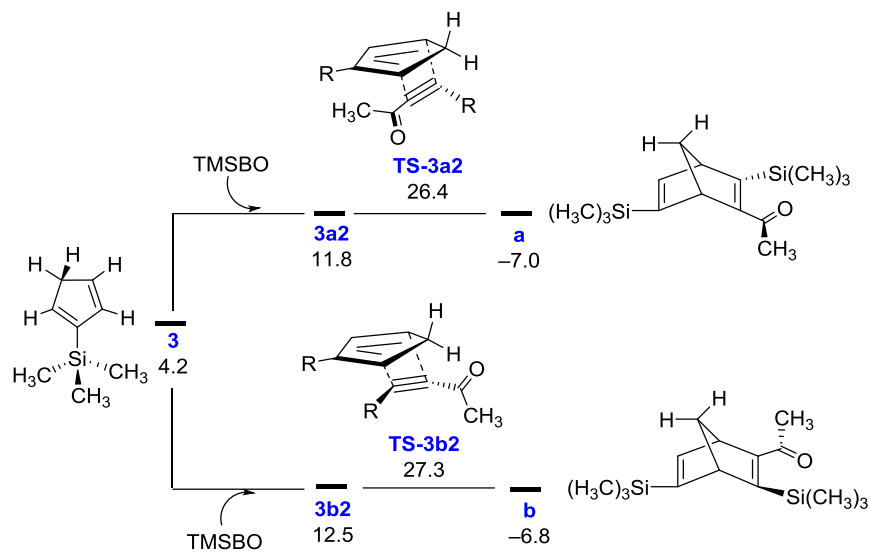


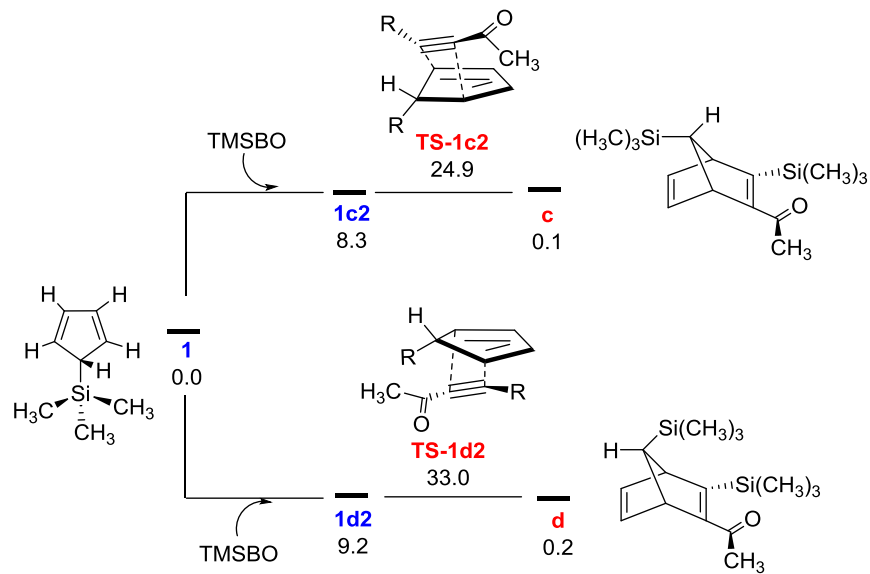
Figure S5. The matched DFT optimized structures with reported X-ray crystal structures (Color green).

(CSD entries: NAWPAE and XALCOE01)²⁰



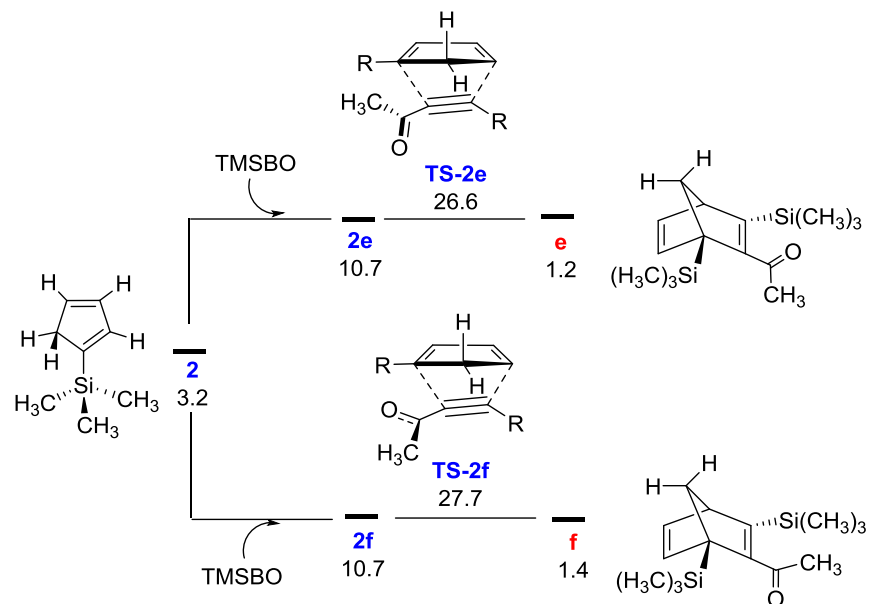
Scheme S4. The second path of Diels-Alder addition of isomer **3** with TMSBO.

TMSBO = 4-(trimethylsilyl)-3-butyn-2-one. R = Si(CH₃)₃. Gibbs energies from (SMD)-PBE/PBEPBE-D3BJ/Def2-TZVP//PBE/PBEPBE-D3BJ/Def2-TZVP computations are given in kcal/mol. Gibbs energies are refer to isomer **1**



Scheme S5. The second path of Diels-Alder addition of isomer **1** with TMSBO.

TMSBO = 4-(trimethylsilyl)-3-butyn-2-one. R = Si(CH₃)₃. Gibbs energies from (SMD)-PBE/PBEPBE-D3BJ/Def2-TZVP//PBE/PBEPBE-D3BJ/Def2-TZVP computations are given in kcal/mol. Gibbs energies are refer to isomer **1**

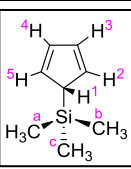


Scheme S6. The path of Diels-Alder addition of isomer **2** with TMSBO.

TMSBO = 4-(trimethylsilyl)-3-butyn-2-one. R = Si(CH₃)₃. Gibbs energies from (SMD)-PBE/PBEPBE-D3BJ/Def2-TZVP//PBE/PBEPBE-D3BJ/Def2-TZVP computations are given in kcal/mol. Gibbs energies are refer to isomer **1**

Table S1. Computed and experimental proton chemical shifts of 1-(C₅H₅)Si(Me)₃ at variable temperatures.

Experimental proton chemical shifts were obtained in neat solvent. The PBE/PBE-D3BJ/Def2-TZVP computed gas-phase proton chemical shifts are given in the Table.

	H1	H2/H5	H3/4	Me ₃
Me ₃ Si(C ₅ H ₅) -10°C	3.29 ppm (6.71 τ)	6.6 ppm (3.4 τ)	6.6 ppm (3.4 τ)	-0.01 ppm (10.01 τ)
Comput -10°C	3.89 ppm	6.79 ppm	6.98 ppm	-0.12 ppm
Me ₃ Si(C ₅ H ₅) 130 °C	5.87 ppm (4.13 τ)	5.87 ppm (4.13 τ)	5.87 ppm (4.13 τ)	-0.01 ppm (10.01 τ)
Comput 130 °C	6.21 ppm	6.21 ppm	6.21 ppm	-0.12 ppm

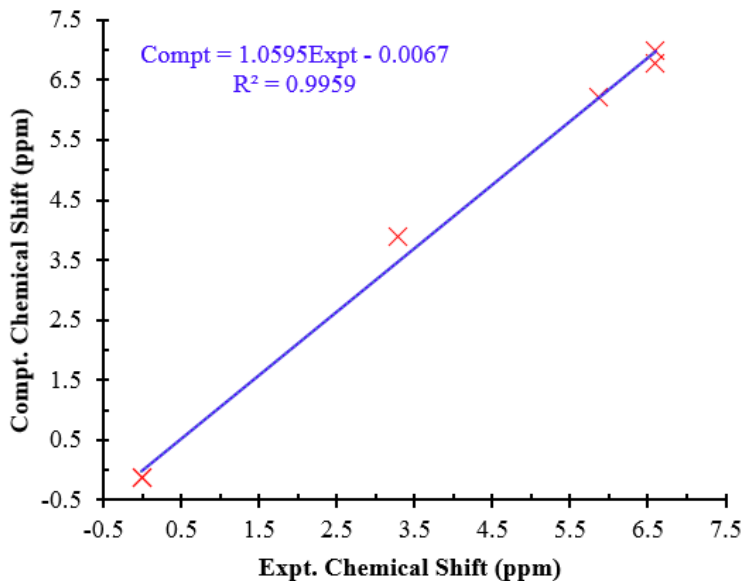


Figure S6. Comparisons of the computed proton chemical shifts and experimental ¹H NMR of 1-(C₅H₅)Si(Me)₃.

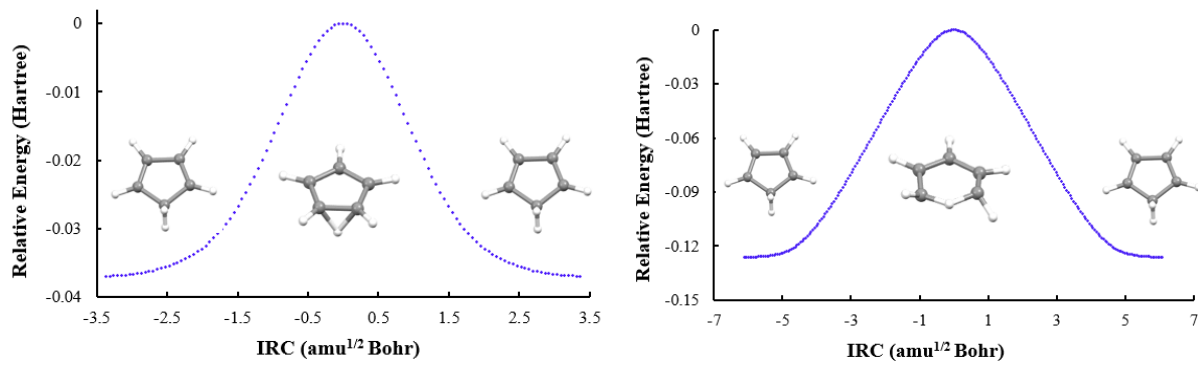


Figure S7. IRC plots for the proton shift in the conversion of cyclopenta-1,3-diene.

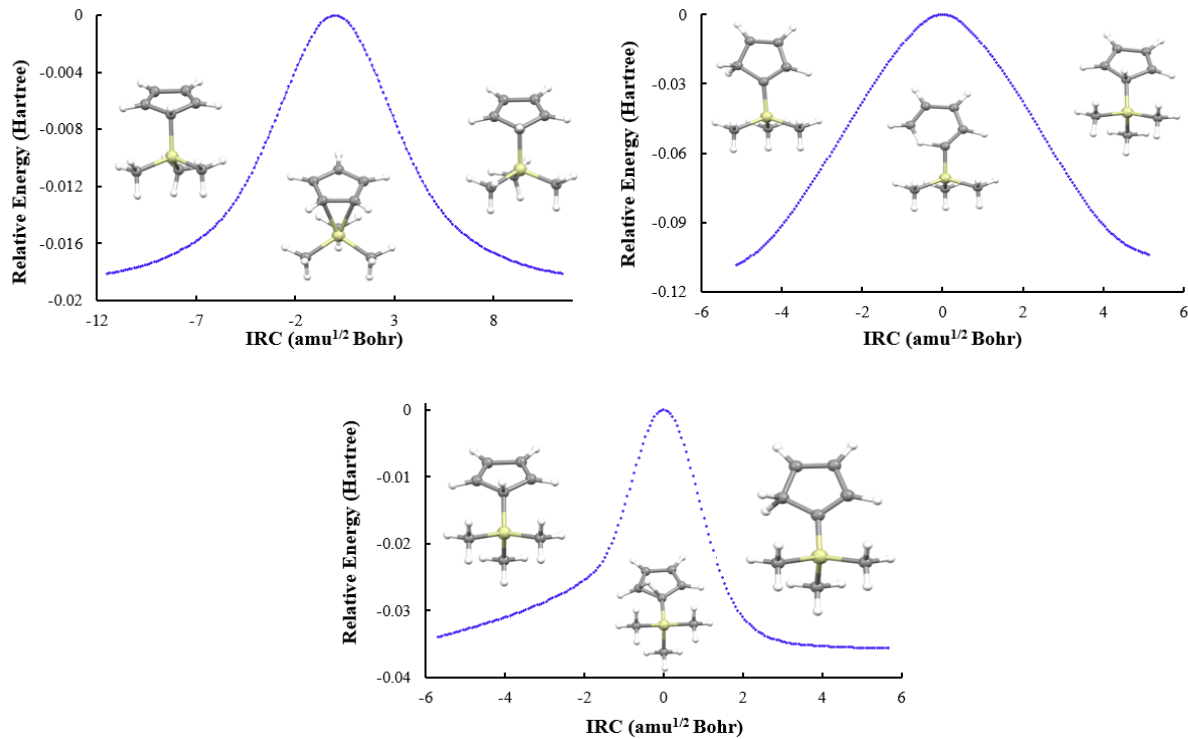


Figure S8. IRC plots for the silicon migration and proton shift in the conversion of 1- $(\text{C}_5\text{H}_5)\text{Si}(\text{Me})_3$.

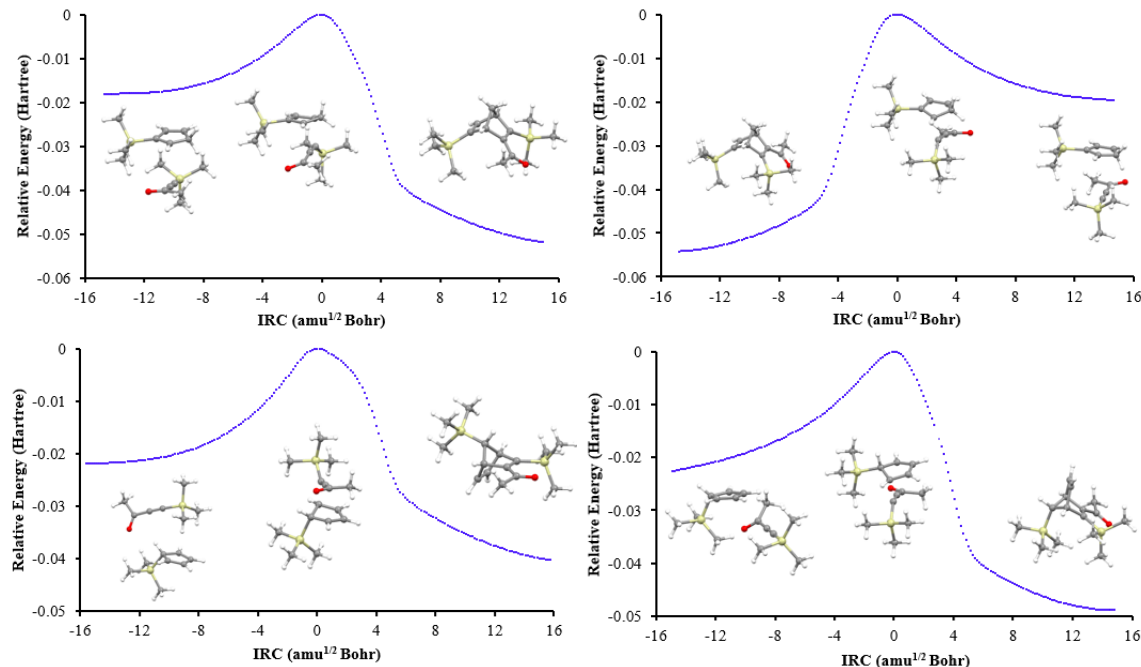


Figure S9. IRC plots for the formation of products **a**, **b**, **c** and **d** from Diels-Alder addition.

Table S2. The selected molecular orbitals of proton shift **TS-1** in cyclopenta-1,3-diene. Isovalue=0.05. Color codes for 3D structures: black, C; white, H.

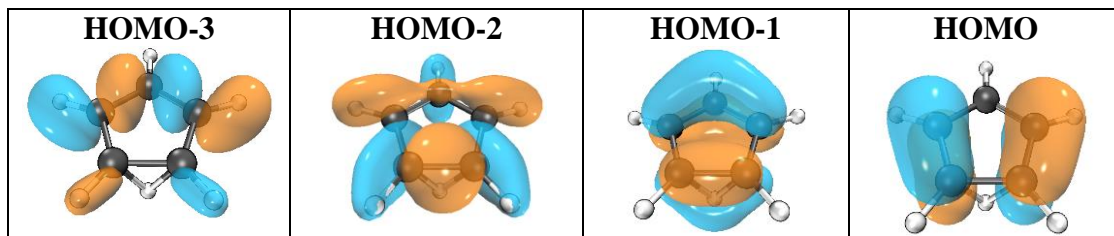


Table S3. The selected molecular orbitals of proton shift **TS-1-i** in cyclopenta-1,3-diene. Isovalue=0.05. Color codes for 3D structures: black, C; white, H.

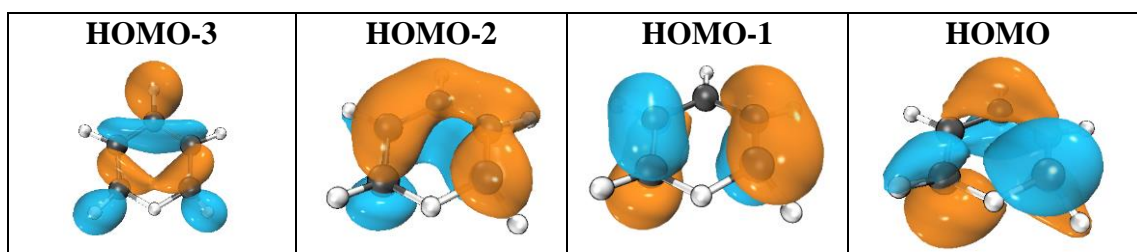


Table S4. DFT optimized structures of 1-(C₅H₅)Si(Me)₃.

Color codes for 3D structures: yellow, Si; gray, C; white, H.

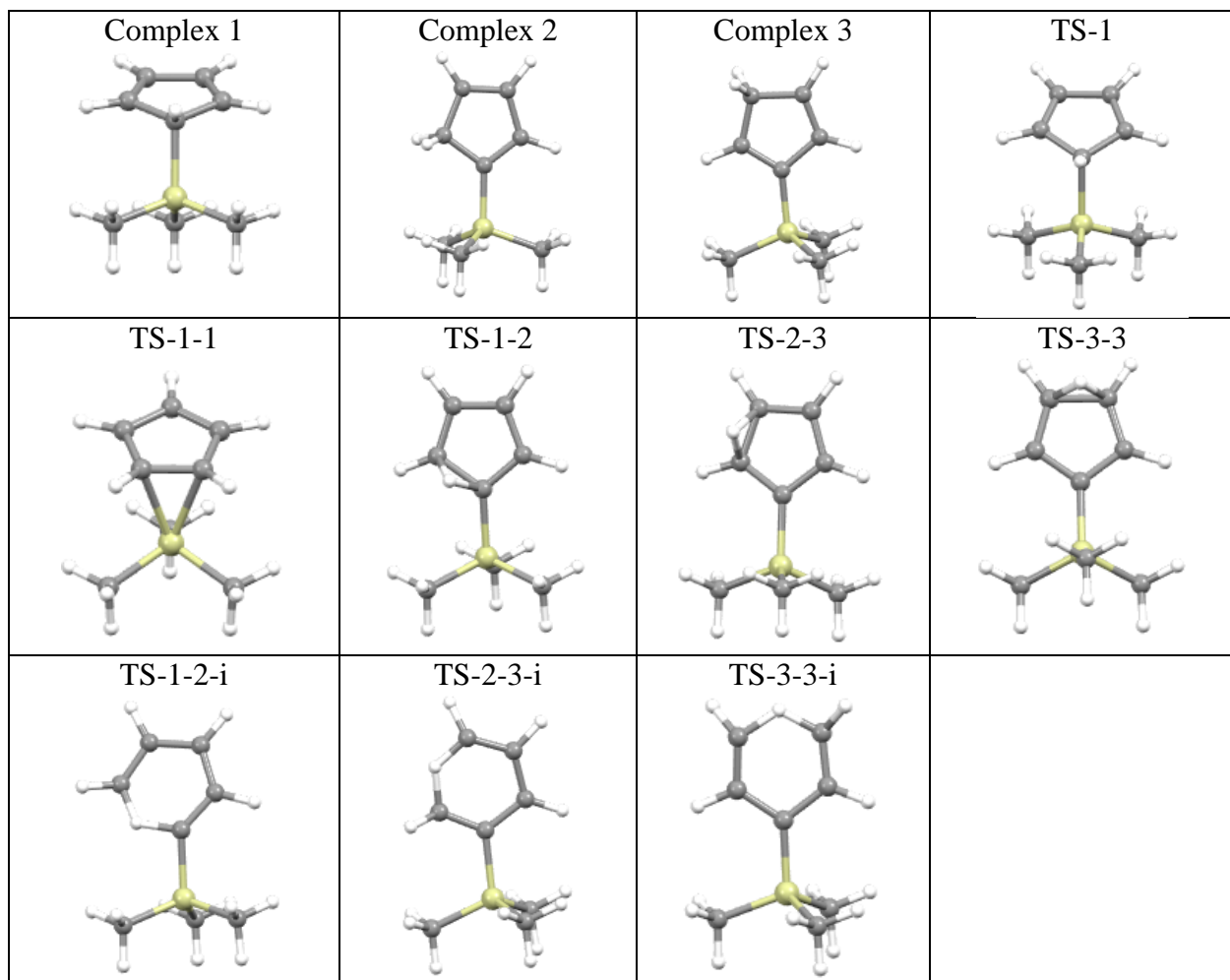


Table S5. The computed relative Gibbs free energies and electronic energies (parentheses) of 1-(C₅H₅)Si(Me)₃.

The PBEPBE-D3BJ/Def2-TZVP computed gas-phase Gibbs free energies and electronic energies (parentheses) are given in kcal/mol.

1	2	3	TS-1	TS-1-1	TS-1-2
0.0	3.1	4.2	6.1	13.3	23.6
(0.0)	(2.4)	(3.6)	(3.7)	(11.5)	(25.1)
TS-2-3	TS-3-3	TS-1-2-i	TS-2-3-i	TS-3-3-i	
24.6	27.0	71.9	75.2	78.0	
(26.2)	(27.3)	(75.6)	(79.6)	(82.1)	

Table S6. The selected molecular orbitals of silicon migration **TS-1-1** in 1-(C₅H₅)Si(Me)₃. Isovalue=0.05. Color codes for 3D structures: yellow, Si; black, C; white, H.

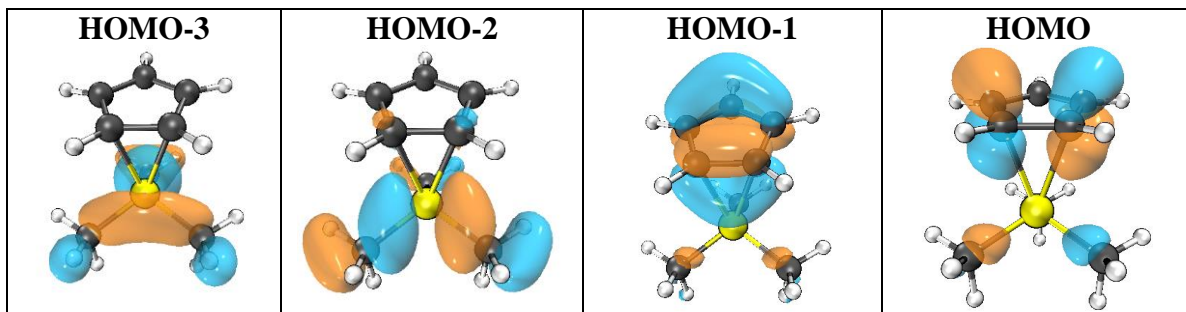


Table S7. The selected molecular orbitals of proton shift **TS-1-2** in 1-(C₅H₅)Si(Me)₃. Isovalue=0.05. Color codes for 3D structures: yellow, Si; black, C; white, H.

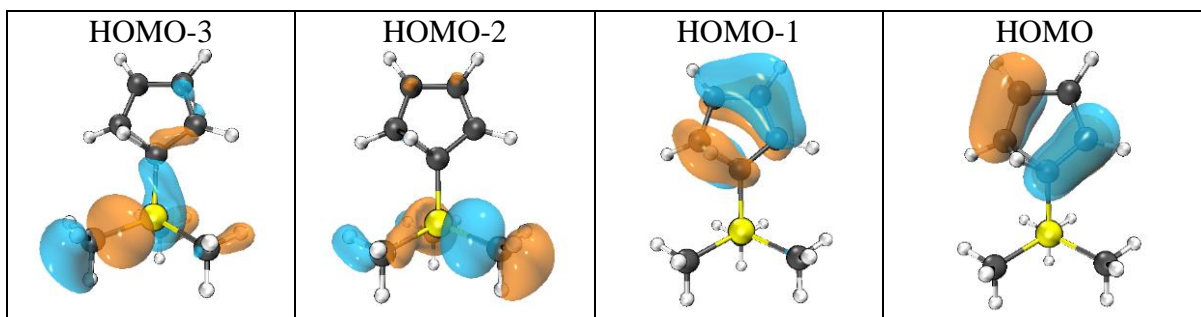


Table S8. The selected molecular orbitals of proton shift **TS-1-2-i** in 1-(C₅H₅)Si(Me)₃. Isovalue=0.05. Color codes for 3D structures: yellow, Si; black, C; white, H.

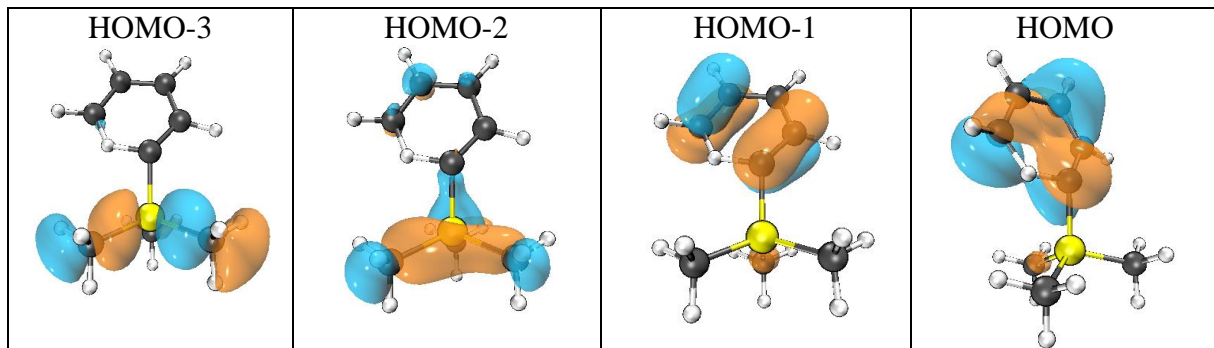


Table S9. The computed relative Gibbs free energies and electronic energies (parentheses) of 1-(C₅H₅)Ge(Me)₃.

The PBEPBE-D3BJ/Def2-TZVP computed gas-phase Gibbs free energies and electronic energies (parentheses) are given in kcal/mol.

1	1-Cs	2	TS-1	TS-1-1	TS-1-2	TS-1-2-i
0.0 (0.0)	0.0 (0.8)	3.8 (4.3)	4.4 (3.0)	10.9 (10.0)	24.3 (26.9)	72.8 (77.7)

Table S10. DFT computed energies for species in **Figures 1 and 2**.

Species	E (PBEPBE-D3BJ/Def2-TZVP)	G (PBEPBE-D3BJ/Def2-TZVP)	E_{soln} (SMD-PBEPBE-D3BJ/Def2-TZVP)
1	-602.343980	-602.194673	-602.351643
2	-602.340093	-602.189775	-602.347631
3	-602.338219	-602.188014	-602.345782
TS-1	-602.338009	-602.184892	-602.345998
TS-1-1	-602.325661	-602.173500	-602.333518
TS-1-2	-602.304005	-602.156992	-602.312435
TS-2-3	-602.302203	-602.155416	-602.310779
TS-3-3	-602.300473	-602.151606	-602.308993
TS-1-2-i	-602.223546	-602.080136	-602.231023
TS-2-3-i	-602.217052	-602.074855	-602.223979
TS-3-3-i	-602.213173	-602.070296	-602.220048
a	-1240.620676	-1240.317372	-1240.632011
b	-1240.621593	-1240.317619	-1240.632539
c	-1240.608683	-1240.305924	-1240.620195
d	-1240.611002	-1240.306533	-1240.621731
e	-1240.605806	-1240.304195	-1240.617351
f	-1240.608047	-1240.304079	-1240.619388
3a	-1240.578396	-1240.286577	-1240.589732
3a2	-1240.578092	-1240.286879	-1240.590086
3b	-1240.577307	-1240.286396	-1240.589887
3b2	-1240.577831	-1240.285834	-1240.589750
1c	-1240.584680	-1240.295201	-1240.595431
1c2	-1240.580252	-1240.291072	-1240.593543
1d	-1240.581918	-1240.291079	-1240.594296
1d2	-1240.580832	-1240.289438	-1240.594384
2e	-1240.579492	-1240.288894	-1240.591225
2f	-1240.579349	-1240.288996	-1240.590969
TS-3a	-1240.560012	-1240.263998	-1240.571675

TS-3a2	-1240.557985	-1240.262607	-1240.570917
TS-3b	-1240.557183	-1240.262052	-1240.570010
TS-3b2	-1240.556460	-1240.260701	-1240.569864
TS-1c	-1240.559861	-1240.264493	-1240.573944
TS-1c2	-1240.558669	-1240.263648	-1240.573007
TS-1d	-1240.552899	-1240.256178	-1240.564847
TS-1d2	-1240.549182	-1240.252133	-1240.562137
TS-2e	-1240.559810	-1240.263019	-1240.572028
TS-2f	-1240.556888	-1240.260415	-1240.569943

References

1. Frisch, M. J.; Trucks, G. W.; Schlegel, H. B.; Scuseria, G. E.; Robb, M. A.; Cheeseman, J. R.; Scalmani, G.; Barone, V.; Mennucci, B.; Petersson, G. A.; Nakatsuji, H.; Caricato, M.; Li, X.; Hratchian, H. P.; Izmaylov, A. F.; Bloino, J.; Zheng, G.; Sonnenberg, J. L.; Hada, M.; Ehara, M.; Toyota, K.; Fukuda, R.; Hasegawa, J.; Ishida, M.; Nakajima, T.; Honda, Y.; Kitao, O.; Nakai, H.; Vreven, T.; Montgomery Jr., J. A.; Peralta, J. E.; Ogliaro, F.; Bearpark, M. J.; Heyd, J.; Brothers, E. N.; Kudin, K. N.; Staroverov, V. N.; Kobayashi, R.; Normand, J.; Raghavachari, K.; Rendell, A. P.; Burant, J. C.; Iyengar, S. S.; Tomasi, J.; Cossi, M.; Rega, N.; Millam, N. J.; Klene, M.; Knox, J. E.; Cross, J. B.; Bakken, V.; Adamo, C.; Jaramillo, J.; Gomperts, R.; Stratmann, R. E.; Yazyev, O.; Austin, A. J.; Cammi, R.; Pomelli, C.; Ochterski, J. W.; Martin, R. L.; Morokuma, K.; Zakrzewski, V. G.; Voth, G. A.; Salvador, P.; Dannenberg, J. J.; Dapprich, S.; Daniels, A. D.; Farkas, Ö.; Foresman, J. B.; Ortiz, J. V.; Cioslowski, J.; Fox, D. J. *Gaussian 09, Revision C.01*. Gaussian, Inc.: Wallingford, CT, USA, 2010.
2. Perdew, J. P.; Burke, K.; Ernzerhof, M. Generalized Gradient Approximation Made Simple. *Phys. Rev. Lett.* **1996**, 77 (18), 3865-3868.
3. Perdew, J. P.; Burke, K.; Ernzerhof, M. ERRATA: Generalized Gradient Approximation Made Simple [Phys. Rev. Lett. 77, 3865 (1996)]. *Phys. Rev. Lett.* **1997**, 78 (7), 1396.
4. Weigend, F.; Ahlrichs, R. Balanced basis sets of split valence, triple zeta valence and quadruple zeta valence quality for H to Rn: Design and assessment of accuracy. *Phys. Chem. Chem. Phys.* **2005**, 7 (18), 3297-3305.
5. Andrae, D.; Häußermann, U.; Dolg, M.; Stoll, H.; Preuß, H. Energy-adjusted ab initio pseudopotentials for the second and third row transition elements. *Theor. Chim. Acta* **1990**, 77 (2), 123-141.
6. Grimme, S.; Antony, J.; Ehrlich, S.; Krieg, H. A consistent and accurate ab initio parametrization of density functional dispersion correction (DFT-D) for the 94 elements H-Pu. *J. Chem. Phys.* **2010**, 132 (15), 154104.
7. Grimme, S.; Ehrlich, S.; Goerigk, L. Effect of the damping function in dispersion corrected density functional theory. *J. Comput. Chem.* **2011**, 32 (7), 1456-1465.
8. Dunlap, B. I. Fitting the Coulomb potential variationally in Xα molecular calculations. *J. Chem. Phys.* **1983**, 78 (6), 3140-3142.
9. Dunlap, B. I. Robust and variational fitting: Removing the four-center integrals from center stage in quantum chemistry. *J. Mol. Struct.: THEOCHEM* **2000**, 529, 37-40.

10. Marenich, A. V.; Cramer, C. J.; Truhlar, D. G. Universal Solvation Model Based on Solute Electron Density and on a Continuum Model of the Solvent Defined by the Bulk Dielectric Constant and Atomic Surface Tensions. *J. Phys. Chem. B* **2009**, *113*, 6378–6396.
11. Lu, T.; Chen, F. Multiwfn: A multifunctional wavefunction analyzer. *J. Comput. Chem.* **2012**, *33* (5), 580-592.
12. Multiwfn, version 3.7, <http://sobereva.com/multiwfn/>. **2020**.
13. Humphrey, W.; Dalke, A.; Schulten, K. VMD: Visual molecular dynamics. *J. Molec. Graphics* **1996**, *14* (1), 33-38.
14. VMD version 1.9.3, <http://www.ks.uiuc.edu/Research/vmd/>. **2016**.
15. Macrae, C. F.; Sovago, I.; Cottrell, S. J.; Galek, P. T. A.; McCabe, P.; Pidcock, E.; Platings, M.; Shields, G. P.; Stevens, J. S.; Towler, M.; Wood, P. A. Mercury 4.0: from visualization to analysis, design and prediction. *J. Appl. Crystallogr.* **2020**, *53* (1), 226-235.
16. The Cambridge Crystallographic Data Centre (CCDC). Mercury version 4.0.0. <http://www.ccdc.cam.ac.uk/mercury/>. **2018**.
17. Ditchfield, R. Self-consistent perturbation theory of diamagnetism. 1. Gauge-invariant LCAO method for N.M.R. chemical shifts. *Mol. Phys.* **1974**, *27* (4), 789-807.
18. Wolinski, K.; Hilton, J. F.; Pulay, P. Efficient Implementation of the Gauge-Independent Atomic Orbital Method for NMR Chemical Shift Calculations. *J. Am. Chem. Soc.* **1990**, *112* (23), 8251-8260.
19. Cheeseman, J. R.; Trucks, G. W.; Keith, T. A.; Frisch, M. J. A Comparison of Models for Calculating Nuclear Magnetic Resonance Shielding Tensors. *J. Chem. Phys.* **1996**, *104* (14), 5497-5509.
20. Ibad, M. F.; Langer, P.; Schulz, A.; Villinger, A. Silylum–Arene Adducts: An Experimental and Theoretical Study. *J. Am. Chem. Soc.* **2011**, *133* (51), 21016-21027.